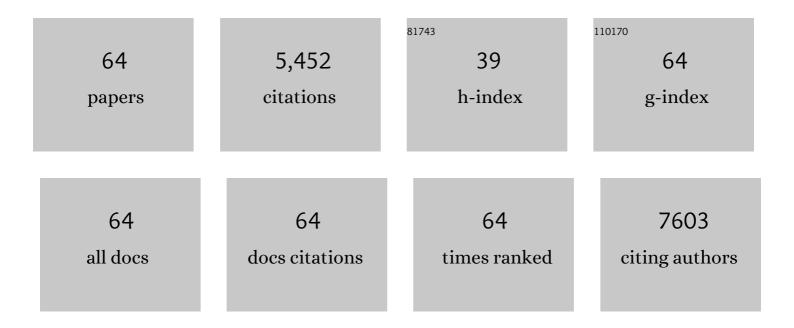
Changhua Wang

List of Publications by Year in descending order

Source: https://exaly.com/author-pdf/728787/publications.pdf Version: 2024-02-01



#	Article	IF	CITATIONS
1	Electrospun Nanofibers of <i>p</i> -Type NiO/ <i>n</i> -Type ZnO Heterojunctions with Enhanced Photocatalytic Activity. ACS Applied Materials & Interfaces, 2010, 2, 2915-2923.	4.0	574
2	Electrospun Nanofibers of ZnOâ^'SnO ₂ Heterojunction with High Photocatalytic Activity. Journal of Physical Chemistry C, 2010, 114, 7920-7925.	1.5	345
3	SnO ₂ Nanostructures-TiO ₂ Nanofibers Heterostructures: Controlled Fabrication and High Photocatalytic Properties. Inorganic Chemistry, 2009, 48, 7261-7268.	1.9	311
4	In situ assembly of well-dispersed gold nanoparticles on electrospun silica nanotubes for catalytic reduction of 4-nitrophenol. Chemical Communications, 2011, 47, 3906.	2.2	276
5	A Facile in Situ Hydrothermal Method to SrTiO ₃ /TiO ₂ Nanofiber Heterostructures with High Photocatalytic Activity. Langmuir, 2011, 27, 2946-2952.	1.6	269
6	Tubular nanocomposite catalysts based on size-controlled and highly dispersed silver nanoparticles assembled on electrospun silicananotubes for catalytic reduction of 4-nitrophenol. Journal of Materials Chemistry, 2012, 22, 1387-1395.	6.7	251
7	ZnO Hollow Nanofibers: Fabrication from Facile Single Capillary Electrospinning and Applications in Gas Sensors. Journal of Physical Chemistry C, 2009, 113, 19397-19403.	1.5	189
8	Electrospinning preparation, characterization and photocatalytic properties of Bi2O3 nanofibers. Journal of Colloid and Interface Science, 2009, 333, 242-248.	5.0	183
9	Synthesis of Natural Cellulose-Templated TiO2/Ag Nanosponge Composites and Photocatalytic Properties. ACS Applied Materials & Interfaces, 2012, 4, 2781-2787.	4.0	144
10	Defect-Induced Yellow Color in Nb-Doped TiO ₂ and Its Impact on Visible-Light Photocatalysis. Journal of Physical Chemistry C, 2015, 119, 16623-16632.	1.5	142
11	TiO2-x/CoOx photocatalyst sparkles in photothermocatalytic reduction of CO2 with H2O steam. Applied Catalysis B: Environmental, 2019, 243, 760-770.	10.8	132
12	Polyacrylonitrile and Carbon Nanofibers with Controllable Nanoporous Structures by Electrospinning. Macromolecular Materials and Engineering, 2009, 294, 673-678.	1.7	119
13	Heterostructured TiO2/WO3 porous microspheres: Preparation, characterization and photocatalytic properties. Catalysis Today, 2013, 201, 195-202.	2.2	118
14	Promotion of multi-electron transfer for enhanced photocatalysis: A review focused on oxygen reduction reaction. Applied Surface Science, 2015, 358, 28-45.	3.1	115
15	Photothermal synergic enhancement of direct Z-scheme behavior of Bi4TaO8Cl/W18O49 heterostructure for CO2 reduction. Applied Catalysis B: Environmental, 2020, 268, 118401.	10.8	115
16	Bi4Ti3O12 nanosheets/TiO2 submicron fibers heterostructures: in situ fabrication and high visible light photocatalytic activity. Journal of Materials Chemistry, 2011, 21, 6922.	6.7	113
17	Hydrothermal Growth of Layered Titanate Nanosheet Arrays on Titanium Foil and Their Topotactic Transformation to Heterostructured TiO ₂ Photocatalysts. Journal of Physical Chemistry C, 2011, 115, 22276-22285.	1.5	111
18	Waterâ^'Dichloromethane Interface Controlled Synthesis of Hierarchical Rutile TiO ₂ Superstructures and Their Photocatalytic Properties. Inorganic Chemistry, 2009, 48, 1105-1113.	1.9	92

Changhua Wang

#	Article	IF	CITATIONS
19	Ti3+ defect mediated g-C3N4/TiO2 Z-scheme system for enhanced photocatalytic redox performance. Applied Surface Science, 2018, 448, 288-296.	3.1	89
20	Enhanced Solar Photothermal Catalysis over Solution Plasma Activated TiO ₂ . Advanced Science, 2020, 7, 2000204.	5.6	89
21	Surface oxygen vacancies on WO3 contributed to enhanced photothermo-synergistic effect. Applied Surface Science, 2017, 391, 654-661.	3.1	85
22	Photoelectrochemical Water Splitting with Rutile TiO2 Nanowires Array: Synergistic Effect of Hydrogen Treatment and Surface Modification with Anatase Nanoparticles. Electrochimica Acta, 2014, 130, 290-295.	2.6	84
23	Simple Ethanol Impregnation Treatment Can Enhance Photocatalytic Activity of TiO ₂ Nanoparticles under Visible-Light Irradiation. ACS Applied Materials & Interfaces, 2015, 7, 7752-7758.	4.0	78
24	Solar photocatalytic activities of porous Nb-doped TiO2 microspheres prepared by ultrasonic spray pyrolysis. Solid State Sciences, 2012, 14, 139-144.	1.5	77
25	Revisiting Pt/TiO ₂ photocatalysts for thermally assisted photocatalytic reduction of CO ₂ . Nanoscale, 2020, 12, 7000-7010.	2.8	73
26	Enhanced photoelectrochemical performance of nanoporous BiVO4 photoanode by combining surface deposited cobalt-phosphate with hydrogenation treatment. Electrochimica Acta, 2016, 195, 51-58.	2.6	66
27	Fabrication, structure, and enhanced photocatalytic properties of hierarchical CeO2 nanostructures/TiO2 nanofibers heterostructures. Materials Research Bulletin, 2010, 45, 1406-1412.	2.7	64
28	Multi-heterojunction photocatalysts based on WO3 nanorods: Structural design and optimization for enhanced photocatalytic activity under visible light. Chemical Engineering Journal, 2014, 237, 29-37.	6.6	63
29	Growth of single-crystalline rutile TiO2 nanowire array on titanate nanosheet film for dye-sensitized solar cells. Journal of Materials Chemistry, 2012, 22, 6389.	6.7	62
30	A novel preparation of three-dimensionally ordered macroporous M/Ti (M=Zr or Ta) mixed oxide nanoparticles with enhanced photocatalytic activity. Journal of Colloid and Interface Science, 2006, 301, 236-247.	5.0	60
31	Thermal coupled photoconductivity as a tool to understand the photothermal catalytic reduction of CO2. Chinese Journal of Catalysis, 2020, 41, 154-160.	6.9	59
32	Rutile TiO2 nanowires on anatase TiO2 nanofibers: A branched heterostructured photocatalysts via interface-assisted fabrication approach. Journal of Colloid and Interface Science, 2011, 363, 157-164.	5.0	50
33	Decorating hierarchical Bi2MoO6 microspheres with uniformly dispersed ultrafine Ag nanoparticles by an in situ reduction process for enhanced visible light-induced photocatalysis. Colloids and Surfaces A: Physicochemical and Engineering Aspects, 2013, 425, 99-107.	2.3	50
34	Rutile TiO2 nanowire array infiltrated with anatase nanoparticles as photoanode for dye-sensitized solar cells: enhanced cell performance via the rutile–anatase heterojunction. Journal of Materials Chemistry A, 2013, 1, 3309.	5.2	49
35	Enhanced electrochromic properties of a TiO ₂ nanowire array via decoration with anatase nanoparticles. Journal of Materials Chemistry C, 2014, 2, 7891.	2.7	47
36	Photoreduced nanocomposites of graphene oxide/N-doped carbon dots toward all-carbon memristive synapses. NPG Asia Materials, 2020, 12, .	3.8	47

#	Article	IF	CITATIONS
37	Coexistence of an anatase/TiO2(B) heterojunction and an exposed (001) facet in TiO2 nanoribbon photocatalysts synthesized via a fluorine-free route and topotactic transformation. Nanoscale, 2014, 6, 5329.	2.8	46
38	Control over energy level match in Keggin polyoxometallate-TiO2 microspheres for multielectron photocatalytic reactions. Applied Catalysis B: Environmental, 2018, 234, 79-89.	10.8	46
39	Morphologically-tunable TiO2 nanorod film with high energy facets: green synthesis, growth mechanism and photocatalytic activity. Nanoscale, 2012, 4, 5023.	2.8	44
40	Photocatalytic activities of heterostructured TiO2-graphene porous microspheres prepared by ultrasonic spray pyrolysis. Journal of Alloys and Compounds, 2014, 584, 180-184.	2.8	39
41	W-Doped TiO ₂ for photothermocatalytic CO ₂ reduction. Nanoscale, 2020, 12, 17245-17252.	2.8	37
42	One-step sol–gel preparation and enhanced photocatalytic activity of porous polyoxometalate–tantalum pentoxide nanocomposites. Journal of Colloid and Interface Science, 2007, 308, 208-215.	5.0	36
43	Simple route to self-assembled BiOCI networks photocatalyst from nanosheet with exposed (001) facet. Micro and Nano Letters, 2012, 7, 152.	0.6	35
44	Synergic effects of Cu O electron transfer co-catalyst and valence band edge control over TiO2 for efficient visible-light photocatalysis. Chinese Journal of Catalysis, 2017, 38, 2120-2131.	6.9	30
45	Correlation between band alignment and enhanced photocatalysis: a case study with anatase/TiO ₂ (B) nanotube heterojunction. Dalton Transactions, 2015, 44, 13331-13339.	1.6	29
46	Three-dimensional hierarchical CeO2 nanowalls/TiO2 nanofibers heterostructure and its high photocatalytic performance. Journal of Sol-Gel Science and Technology, 2010, 55, 105-110.	1.1	28
47	Synergistic effect of surface self-doping and Fe species-grafting for enhanced photocatalytic activity of TiO2 under visible-light. Applied Surface Science, 2017, 396, 26-35.	3.1	28
48	Solution plasma boosts facet-dependent photoactivity of decahedral BiVO4. Chemical Engineering Journal, 2020, 397, 125381.	6.6	28
49	Bi4TaO8Cl/Bi heterojunction enables high-selectivity photothermal catalytic conversion of CO2-H2O flow to liquid alcohol. Chemical Engineering Journal, 2022, 435, 135133.	6.6	27
50	Anatase/Bronze TiO2 Heterojunction: Enhanced Photocatalysis and Prospect in Photothermal Catalysis. Chemical Research in Chinese Universities, 2020, 36, 992-999.	1.3	26
51	Photoluminescence properties of highly dispersed ZnO quantum dots in polyvinylpyrrolidone nanotubes prepared by a single capillary electrospinning. Journal of Chemical Physics, 2008, 129, 114708.	1.2	23
52	Bilayer TiO ₂ photoanode consisting of a nanowire–nanoparticle bottom layer and a spherical voids scattering layer for dye-sensitized solar cells. New Journal of Chemistry, 2015, 39, 4845-4851.	1.4	23
53	The W@WO ₃ ohmic contact induces a high-efficiency photooxidation performance. Dalton Transactions, 2017, 46, 1487-1494.	1.6	18
54	Revisiting cocatalyst/TiO2 photocatalyst in blue light photothermalcatalysis. Catalysis Today, 2019, 335, 286-293.	2.2	16

Changhua Wang

#	Article	IF	CITATIONS
55	TiO2 (B) nanosheets mediate phase selective synthesis of TiO2 nanostructured photocatalyst. Applied Surface Science, 2014, 292, 937-943.	3.1	14
56	High-humidity tolerance of porous TiO2(B) microspheres in photothermal catalytic removal of NO. Chinese Journal of Catalysis, 2020, 41, 1622-1632.	6.9	14
57	Three-dimensionally ordered macroporous Tilâ^'xTaxO2+x/2 (x=0.025, 0.05, and 0.075) nanoparticles: Preparation and enhanced photocatalytic activity. Materials Letters, 2006, 60, 2711-2714.	1.3	13
58	Transparent Nb-doped TiO ₂ films with the [001] preferred orientation for efficient photocatalytic oxidation performance. Dalton Transactions, 2017, 46, 15363-15372.	1.6	13
59	Elucidation of the electron energy structure of TiO ₂ (B) and anatase photocatalysts through analysis of electron trap density. RSC Advances, 2020, 10, 18496-18501.	1.7	11
60	Vacuum heat treated titanate nanotubes for visible-light photocatalysis. New Journal of Chemistry, 2015, 39, 1281-1286.	1.4	9
61	Ultrasonic spray pyrolysis assembly of a TiO2–WO3–Pt multi-heterojunction microsphere photocatalyst using highly crystalline WO3 nanosheets: less is better. New Journal of Chemistry, 2016, 40, 3225-3232.	1.4	8
62	Minimization of defects in Nb-doped TiO 2 photocatalysts by molten salt flux. Ceramics International, 2018, 44, 10249-10257.	2.3	8
63	Efficiency enhanced rutile TiO2 nanowire solar cells based on an Sb2S3 absorber and a CuI hole conductor. New Journal of Chemistry, 2015, 39, 7243-7250.	1.4	7
64	One-Step Nonaqueous Synthesis of Pure Phase TiO ₂ Nanocrystals from TiCl ₄ in Butanol and Their Photocatalytic Properties. Journal of Nanomaterials, 2011, 2011, 1-6.	1.5	5